Multichannel Nerve Stimulation for Diverse Activation of Finger Flexors

Henry Shin and Xiaogang Hu

***Abstract*— *Objective*: Neuromuscular electrical stimulation (NMES) is a common approach to restore muscle strength of individuals with a neurological injury but restoring hand dexterity is still a challenge. This study sought to quantify the diversity of finger movements elicited by a multichannel nerve stimulation technique. *Methods*: A 2 × 8 stimulation grid, placed on the upper arm along the ulnar and median nerves, was used to activate different finger flexors by automatically switching between randomized bipolar electrodes. The forces from each individual finger as well as the high-density electromyogram (HDEMG) of the intrinsic and extrinsic flexors were recorded. The elicited finger forces were categorized using hierarchical clustering, and the 2D correlation of the spatial patterns of muscle activation was also calculated. *Results*: A wide range of movement patterns were identified, including multi-finger and single-digit movements. Additionally, a number of electrode pairs elicited similar finger movements. The muscle activation patterns showed similar and distinct spatial patterns, signifying activation redundancy. *Conclusion*: These results revealed the diversity of elicitable finger movements and muscle activations. The system redundancy can be explored to compensate for system instability due to fatigue or electrode shift. The outcomes can also enable the development of an automatic calibration of the stimulation.**

***Index Terms*— Neuromuscular electrical stimulation, neuroprosthesis, finger dexterity, hand function, finger flexion.**

I. Introduction

WEAKNESS of the hand is a major contributor to the loss of self-sufficiency and independence following a neurological injury such as a stroke [1]–[3] or a spinal cord injury [4], [5]. The loss of the descending drive to the muscles is typically the main initial cause of the paresis [6], but paresis associated complications, including disuse and further atrophy, can aggravate the loss of strength. Neuromuscular electrical stimulation (NMES) is a commonly utilized tool to augment muscle activation and to restore functions of the hand [7]–[10]. Although conventional electrical stimulation methods have shown benefits in increased grip strength and object manipulation [11]–[13], NMES techniques still face various limitations in their specificity and selectivity of different finger movement patterns.

Manuscript received January 8, 2019; revised June 14, 2019 and September 20, 2019; accepted October 11, 2019. Date of publication October 14, 2019; date of current version December 6, 2019. This work was supported by the National Science Foundation under Grant CBET1847319. *(Corresponding author: Xiaogang Hu.)*

The authors are with the UNC/NCSU Joint Department of Biomedical Engineering, Chapel Hill, NC 27514 USA (e-mail: xiaogang@unc.edu).

Digital Object Identifier 10.1109/TNSRE.2019.2947785

Conventional NMES uses large electrodes placed on the skin near the motor points of the targeted muscles to deliver electrical stimulation and induce muscle-specific movements. For finger flexion NMES, these electrodes are typically placed on the anterior compartments of the forearm and are often only able to elicit gross grasp patterns involving all the fingers. Recent developments to improve the specificity and range of motions in the hand have focused on using multi-electrode grids to distribute the stimulation across different muscles or muscle regions [14]–[16]. For example, a wearable hand NMES system developed by Crema et al. utilizes electrode arrays across the hand and forearm to selectively control the hand [17].

An alternative method for NMES is the stimulation of the more proximal nerve bundles. Several studies have demonstrated that proximal nerve stimulation in the lower limb can better involve central pathways, which can also delay fatigue onset [18]–[20]. For finger flexion, the ulnar and median nerve bundles are superficially accessible near the biceps brachii. Previous studies have shown that stimulation in this region is able to elicit a variety of finger movement patterns which include both single finger and multi-finger activation [21], and some preliminary studies on the use of a multi-electrode array to select movement patterns have demonstrated the selective capabilities of this method [22]–[24]. Stimulation of the proximal nerve bundle has also shown the ability to delay muscle fatigue onset [25]–[27].

However, the multi-electrode array either targeting the muscle belly or the nerve bundle typically relay on manual search for a single electrode pair which elicits a desirable motion. As a result, the determination of which set of electrodes is best to use for a desired motion is non-trivial, and inter-session replication still requires extensive stimulation and motion identification every time the electrode arrays are replaced. This electrode array characterization is therefore a common feature of multi-electrode systems and necessitates automated calibration methods for streamlined usage [28]. A broader characterization of the stimulation method and the available movement patterns as well as its repeatability across subjects has not been investigated.

Accordingly, the objective of the current study was to quantify the types of finger flexion patterns elicited through the multi-electrode array by utilizing an automated electrode search procedure. The forces from individual fingers were obtained to quantify the movement patterns. High-density electromyogram (HDEMG) on the palm and on the anterior forearm were recorded to capture both intrinsic and extrinsic

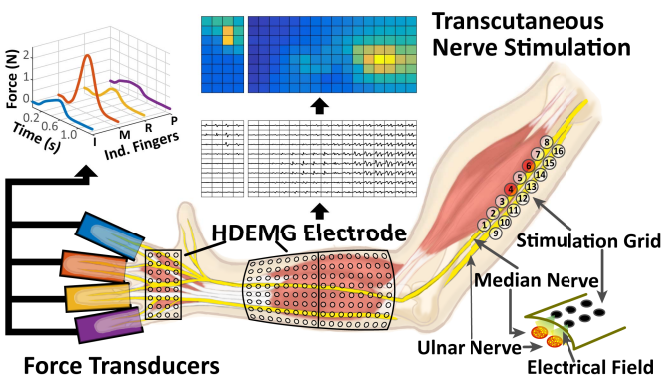

Fig. 1. Overview of Experimental Setup. A stimulation grid of electrodes (right) along the ulnar and median nerves was used to selectively activate unique patterns of finger flexion forces. The motor activity from each pair of electrodes was recorded using individual force transducers (left) and an array of high-density EMG electrodes (middle). Samples of data are also shown. Each stimulation through an electrode pair elicits a unique force profile and set of HDEMG activity which can also be simplified as a heat map (top).

muscle activities. The 2D correlation of the spatial patterns of muscle activation was calculated to assess the redundancy of the system. Our results revealed a diverse set of finger flexion patterns. This catalogue and automatic detection of available finger forces can establish a basis for further development of an NMES system for rehabilitation and functional assistance.

II. Methods

Eight neurologically intact subjects (6 males, 2 females, 20-34 years of age) without any known neurological conditions were recruited. All subjects gave informed consent with protocols approved by the Institutional Review Board of the University of North Carolina at Chapel Hill.

A. Electrical Stimulation Generation

A 2×8 grid of individual round electrodes (1 cm diameter) was placed near the biceps brachii on the medial side of the arm where the ulnar and median nerves are located just below the skin (Figure 1). The grid of electrodes was aligned parallel to the nerve bundles, and each electrode was placed on average ∼1.5 cm apart from each other. Each electrode was routed through a switch matrix (34904A, Agilent Technologies), and all stimulation was delivered using an 8-channel programmable stimulator (STG4008, Multichannel Systems). Stimulation trains could be generated and routed through any pair of electrodes. All stimulation was delivered in biphasic pulses with a 500 μs pulse width, and a pulse frequency of 30 Hz.

B. Automated Stimulation and Motor Activity Recording

The resultant EMG and force elicited by the electrical stimulation was recorded as a measure of motor activity (Figure 1). An 8×16 HDEMG array (ELSCH064NM3, OT Bioelettronica) was placed over the extrinsic flexor muscles of the hand. An 8×4 HDEMG array was also placed on the palm over the intrinsic hand muscles. Ground and subject reference electrode bands were placed around the wrist and elbow, respectively. All 160 monopolar EMG channels were amplified at a gain of 200, filtered at 2-900 Hz, and sampled at 5120 Hz (EMG-USB2+, OT Bioelettronica). The force of each individual finger was also recorded through four separate 100 N force transducers (SM-100N, Interface Inc.), which were individually fixed to each finger using custom 3D printed cradles. The force signal was sampled at 1000 Hz. The EMG and force was recorded synchronously with the electrical stimulation. To improve the efficiency of searching through the stimulation electrode grid, the electrical stimulation generation, switch matrix control, and EMG/force acquisition were all fully automated via a custom-made MATLAB user interface. This overall procedure is illustrated in Figure 2A. The stimulator was connected to a randomly selected pair of stimulation electrodes. Bipolar, charge-balanced electrical stimulation was generated across the electrode pair, and the EMG and force signals were simultaneously triggered to sample for the duration of the electrical stimulation. A 0.5 second of electrical stimulation was delivered per electrode pair to allow force accumulation, which was repeated 3 times with 1 second of rest between stimulation. From each set (0.5 second) of stimulation pulse trains, the elicited compound muscle action potential (CMAP) could be isolated from the EMG signal between stimulus times. For each stimulation, the individual finger forces were also obtained during the total 1.5 second duration of the stimulation and rest time. This set of CMAP EMG activity, four finger forces, and stimulation parameters was recorded for every available combination of stimulation electrode pairs in the 2×8 stimulation grid (a maximum of 120 combinations).

C. Procedure

Subjects were seated in front of the force transducers. An initial current stimulation (4 mA) was used to determine and disable any individual electrode which elicited a strong noxious sensation local to the stimulation site. Of the 16 stimulation electrode sites, one subject had three electrodes removed, two subjects had one electrode removed, and the remaining 5 had no electrodes that induced noxious sensation. The HDEMG electrode arrays were then placed on the forearm and hand. The wrist was prevented from applying force to the transducers by holding the palm and forearm in a neutral position between Styrofoam-covered U-shaped wooden blocks, secured to the table. Once the fingers and wrist were all secure, the subject was requested to produce maximum voluntary contractions (MVCs) of each individual finger. Following the MVCs, the automated switch-stimulator system was initiated to cycle through every available combination of stimulator electrode pairs at an initial current of 3 or 4 mA. The default current of 4 mA was used in most cases. If there were pronounced flexion forces of all the fingers above 50% MVC, which resulted in a single strong force pattern from all of the fingers, an initial current of 3 mA was used in 3 of 8 subjects.

Upon completion of the initial search, the pair of electrodes which produced the strongest average peak force was selected as a representative electrode pair for further testing. This pair was used to estimate the current-force relation of the

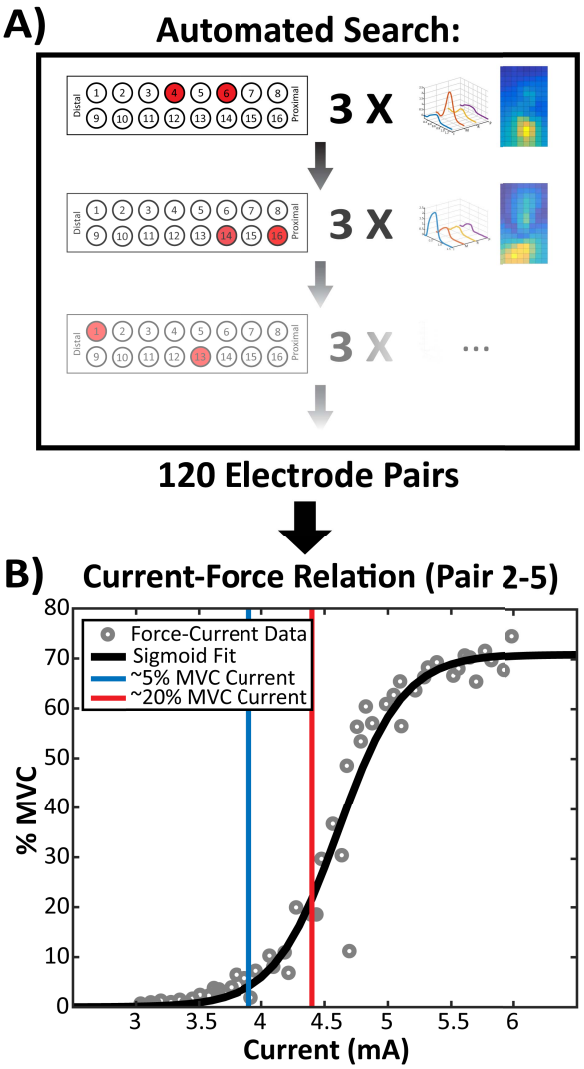

Fig. 2. Search Procedure Diagram. A) Depiction of the automated search procedure. Each stimulation electrode pair is repeated 3 times while recording the resultant EMG and force. B) After the initial search, a current-force relation is obtained at the electrode pair which elicited the maximum force. Each current-force data point is plotted live for the experimenter, and the sigmoidal fit (black line) is calculated and overlaid on the data. Two current values were identified which matched 5% (blue) and 20% (red) activation levels for further automated grid searching.

whole grid, and to obtain the current value which corresponded to ~5% and ~20% of the averaged MVC (Figure 2B). These two levels were selected as a general estimate of low and medium finger forces which could be expected during daily usage of the hand [29]. To obtain the current values needed to stimulate these force levels, the switch matrix was first manually set to the strongest electrode pair. Then, the electrode pair was stimulated at manually selected current levels to determine both the minimum motor threshold current and a maximum current level which corresponded to a stable plateau force above 50% of MVC. But if the high current intensity caused skin discomfort, a range from 0 to 50% MVC force output was still obtained. Once these two boundary levels were determined, another automated stimulation protocol was initiated to stimulate at 50 pseudo-random current amplitudes between the upper and lower current levels. In order to prevent fatigue, the electrodes were stimulated for 0.5 seconds, and 3 seconds of rest was provided between stimulations. The averaged peak forces of each stimulation were recorded and displayed to construct the current-force function seen in Figure 2B. Once completed, the experimenter used the current-force function to estimate the current levels which can elicit the desired 5% and 20% MVC. These two current levels represented the low and medium activation levels.

The final sets of automated electrode pair searching were then initiated at the 5% and 20% MVC current levels. The order of the low and medium current was randomized between subjects. Each electrode pair was stimulated 3 times (0.5 second active, 1 second rest) before switching to the next pair, and all EMG and forces were recorded simultaneously. Each set of stimulation at each current level was separated by a minimum of 1 minute of rest, and none of the subjects reported any fatigue or muscle strain upon completion.

D. Data Processing

For every stimulated electrode pair at each current level, the corresponding forces and EMG data were segmented for the duration of every half second of stimulation. The forces and EMG obtained from each electrode pair were hereby referred to as a stimulation set. The force of each stimulation set was averaged across the 3 repetitions to obtain a single force activity profile of the 4 fingers. The force profile was then smoothed using a 100 ms moving window (1 ms step).

Additionally, the EMG data following each stimulation pulse were extracted for every EMG channel, and then averaged across the entire stimulation set. The first 2 ms post stimulation was excluded to remove the stimulus artifact, and the subsequent 30 ms of EMG were extract. These isolated CMAPs included both the characteristic M-wave and H-reflex. To quantify the overall level of activation, the Area-under-the-Curve (AUC) was calculated from the average of the absolute value of each post-stimulation EMG to represent the overall activity of a single channel (units: mV-ms). These values from all the EMG channels were combined to form activation heat maps (Figure 1). Each heat map represents the overall HDEMG activity for a given electrode pair and current level.

In summary, the data acquisition and processing resulted in every electrode pair (120 maximum) and current level (Initial, 5%, 20%) to have its own corresponding force and EMG activity profile per subject. Any stimulation sets which produced less than 1% MVC force on all four fingers were excluded from subsequent analyses. The percentage (Mean ± SD) of excluded electrode combinations was 30.1 ± 11.5%

E. Data Clustering and Analysis

To quantify the available activity across the stimulation grid, hierarchical clustering was used to categorize the force profiles. Clustering of the force data was selected over the EMG data as the force data produced more visually intuitive clusters that could be directly related to the movements of the hand. Specifically, all the force profiles from a single subject were pooled together, regardless of the current level. Each set of force data can be considered a 2D array of

the 4 finger forces sampled at 1000 Hz over each 0.5 s of stimulation. Rather than reducing the forces to a single value, the 2D correlation coefficient was calculated between every force profile to compare the overall shape of the force generated over time. This correlation value represented the force profile distance between electrode pairs, and the complement (1 – Distance) was calculated to obtain the dissimilarity matrix needed for clustering. The MATLAB hierarchical clustering function *cluster()* was used with the standard inconsistency cutoff of 1.1 to form initial force clusters. For further optimization, the silhouette (SIL) coefficient was first calculated for every cluster member. The SIL is a measure of cluster validity which compares the average within-cluster distance of a data point with that of its closest neighboring cluster [30]. A SIL value close to +1 indicates an appropriately clustered data point, whereas a SIL value close to -1 indicates that the data point is a better fit in a different cluster. The cluster groupings were optimized to maximize the SIL score of each group by reassigning any force profile with a negative SIL to a better (higher SIL) cluster group. If no non-negative SIL group was possible, the force profile was used to form its own new cluster, and the SIL was recalculated for all other data points. This process was repeated iteratively until the cluster members converged to a stable grouping. Lastly, once these final cluster groups were found, the averaged force profile of each cluster was calculated to represent the force of the cluster. The ratio of finger activation of each force profile was used to determine which fingers were most active within the cluster (e.g. Index-Middle), and these were then used as movement labels (e.g. IM) to categorize each force cluster.

The HDEMG AUC maps were also obtained from each cluster. As a measure of the similarity of the EMG activity within each cluster, the 2D correlation between each AUC map was first calculated, and the average correlation within each cluster was used to represent the overall similarity of the EMG activation pattern of each cluster. Separate correlations were calculated for the hand and arm HDEMG arrays. To compare the AUC correlations between the hand and arm across all subjects, the average correlation coefficient values were variance-stabilized using the Fisher z-transformation (z=*arctanh(c)*). A paired t-test was performed to test whether the two EMG locations had similar correlation across subjects.

III. Results

For each subject, the force data were summarized by extracting the normalized peak force of each force profile. The index and middle finger forces were combined and the ring and little finger forces were combined, which represented an average of the activations corresponding to the radial and ulnar sides of the hand (Index-Middle vs Ring-Pinky). Figure 3 shows the finger force patterns of a sample subject at the low (5% MVC) and medium (20% MVC) activation levels across the entire stimulation grid. Each data point represents the force from a single stimulation electrode pair, and the polar angle of each point represents the ratio of the activation between the Index-Middle and the Ring-Pinky finger forces. A more spread or distributed set of data points signified that the elicited

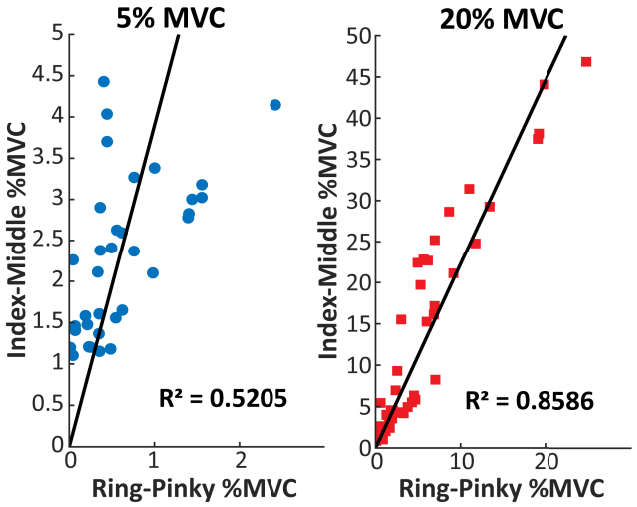

Fig. 3. Sample Force Distribution between the Two Current Levels in a Sample Subject. The peak force from every electrode pair was plotted against the %MVC average of the Index and Middle fingers vs the Ring and Pinky fingers. The spread of the data points illustrates the distribution of activation between each half of the hand, and the best fit line through the origin (black line) was plotted to estimate the overall activation trend of all the fingers.

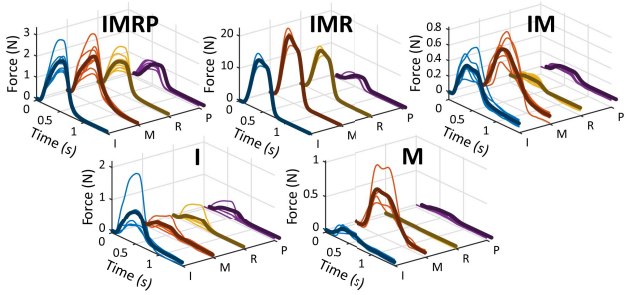

Fig. 4. Sample Force Clusters of a Single Subject. Sample force profiles representing each movement label was chosen from a single subject. Thin lines represent the force profile of individual electrode pair, and the thicker line is the averaged force profile. Movement labels show which fingers were determined to be most active relative to the other fingers.

forces had more varying ratios of activation, indicating one set of fingers could be selectively activated over the other set of fingers. On the other hand, a linear set of points with small deviation from the regression line suggested that the elicited data points had more similar ratios of activation, indicting similar proportions of finger co-activation across all the electrode pairs. The low activation level showed a more distributed range of force levels, which varied from primarily Index-Middle forces to combinations of Ring-Pinky forces with comparable low-medium force levels. The medium activation level showed a more linear range of force activation. Across all subjects, the low activation showed a similar trend of more distributed forces with a median R^2 of 0.65 and an interquartile range of 0.26 while the medium activation levels had a median R^2 of 0.95 and an interquartile range of 0.12.

Samples of force clusters obtained from a representative subject are shown in Figure 4 with the movement labels above each clustered set of electrode pairs. Many of the force clusters

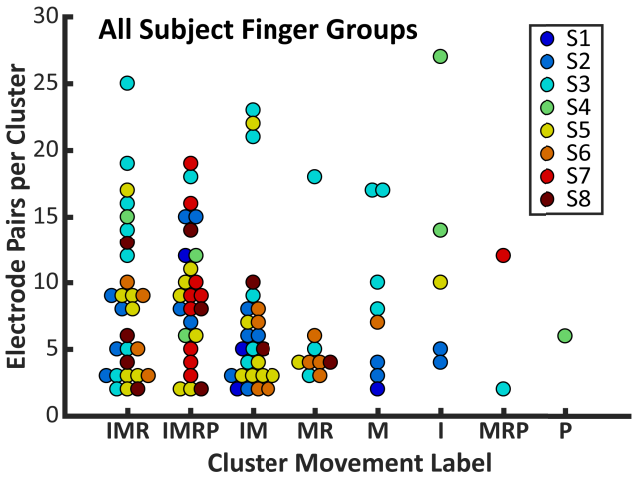

Fig. 5. All Subject Cluster Activity. Each colored circle represents a force cluster obtained from a single subject. The cluster movement label represents which fingers are most active relative to the others within a force cluster. The y-axis location shows the number of electrode pair activations which contribute to the movement cluster.

from this subject involved the Index and Middle fingers, while a smaller proportion additionally activated the Ring and/or Pinky fingers. Although not as common, there are also several candidate clusters which induce only single Index or Middle finger forces. The finger activation patterns based on the force clusters across all the subjects are summarized in Figure 5. Each colored circle represents a single force cluster from a single subject. The movement label of the cluster was used to group each force cluster. Each cluster was then organized from left to right based on the total number of clusters within each movement label group. For each movement pattern, both small and large clusters were observed, which indicated that some sets of electrode pairs produced similar force patterns.

Figure 6A and 6B shows samples of arm AUC maps with either a low or high 2D correlation from a cluster. Each AUC cluster had a variable range of AUC correlation. A high average correlation value suggested that the electrode pairs within the cluster activated similar portions of muscle. In contrast, a low average correlation value suggested that the cluster of electrodes produced similar force outcomes, but through dissimilar muscle activation. The average correlation of all the arm and hand AUC clusters from a single subject are shown in Figure 6C, and the overall interquartile range of AUC correlations for each subject are shown in Figure 6D. A paired t-test between the AUC correlation coefficients showed that the arm and hand correlations are significantly different [$t(7) = 5.88$, $p < 0.05$]. The arm AUC correlations were higher than the hand AUC correlations, suggesting that, within a force cluster, the EMG activity in the arm was usually more similar than the EMG activity in the hand.

IV. Discussion

In the current study, transcutaneous electrical stimulation was delivered to the proximal nerve bundles using a multi-electrode grid system. An automated method was used to record all available activity in the electrode grid at multiple current amplitudes. This activity was then grouped using hierarchical clustering to form intuitively discernable force patterns. Overall, our results demonstrate the capabilities of the current methodology in eliciting a variety of finger activation patterns, but also being able to find different electrode pairs that produced similar force patterns. Understanding the available range of finger activation patterns elicitable through the electrode grid is a necessary step for future automated calibration and selection of stimulation locations.

A. Finger Activation Patterns

Our results show that the proximal nerve electrode grid can target a wide variety of finger forces. Across all subjects, the two most common movement patterns observed in Figure 5 are the Index-Middle-Ring and Index-Middle-Ring-Pinky movements. Both of these multi-finger movements indicate a strong activation of the median nerve with the latter movement suggesting the additional activation of the ulnar nerve to recruit the Ring and Pinky fingers. These two movements are functionally related to whole hand grasping and other similar power grasps necessary for holding or moving objects. These results are also similar to grasp patterns elicited in our previous kinematic study [21]. After those two patterns, the next common movements of double or single fingers represent a selective activation of nerve fibers within the nerve bundle. The electrode pairs which elicit these movements are selective to a specific set of fingers which functionally represent fine movements and pinch grasps [31].

Comparatively, the hand NMES system developed by Crema et al. represents the current state-of-the-art of multi-electrode array for motor point stimulation. This system could selectively control various sets of fingers for functional grasps, by stimulating at different sets of electrodes across the hand and forearm [17]. This study utilizes an initial searching procedure to map the kinematic responses of different electrodes. A combination of specific fingers was then stimulated in sequence to initiate and control various movement patterns, such as pinching, power grasps, and object-specific hand shaping. Although Crema et al. reported that single finger movement could not be achieved with motor point stimulation, the overall success of the method illustrates that coupled movements can still be functionally useful.

Although motor point stimulation has unitary selectivity of function, which is directly related to the underlying muscle, the selectivity of an electrode pair in the current study to a specific set of desired finger forces is both a function of the electrode location relative to the nerve bundles as well as the stimulation intensity. Figure 3 and the median R^2 values lends insight into the effects of the current level on grasp selectivity. At lower current-force levels, the distribution of generated forces is less linear (lower R^2) than at higher current levels. These values suggest that the individual electrode pairs can elicit more varied or flexible activation of different fingers. Physiologically, the lower current-force level may activate a smaller number of nerve fibers, leading to finger-specific movements. As the current is increased, more nerve fibers are recruited, which leads to a more similar activation of

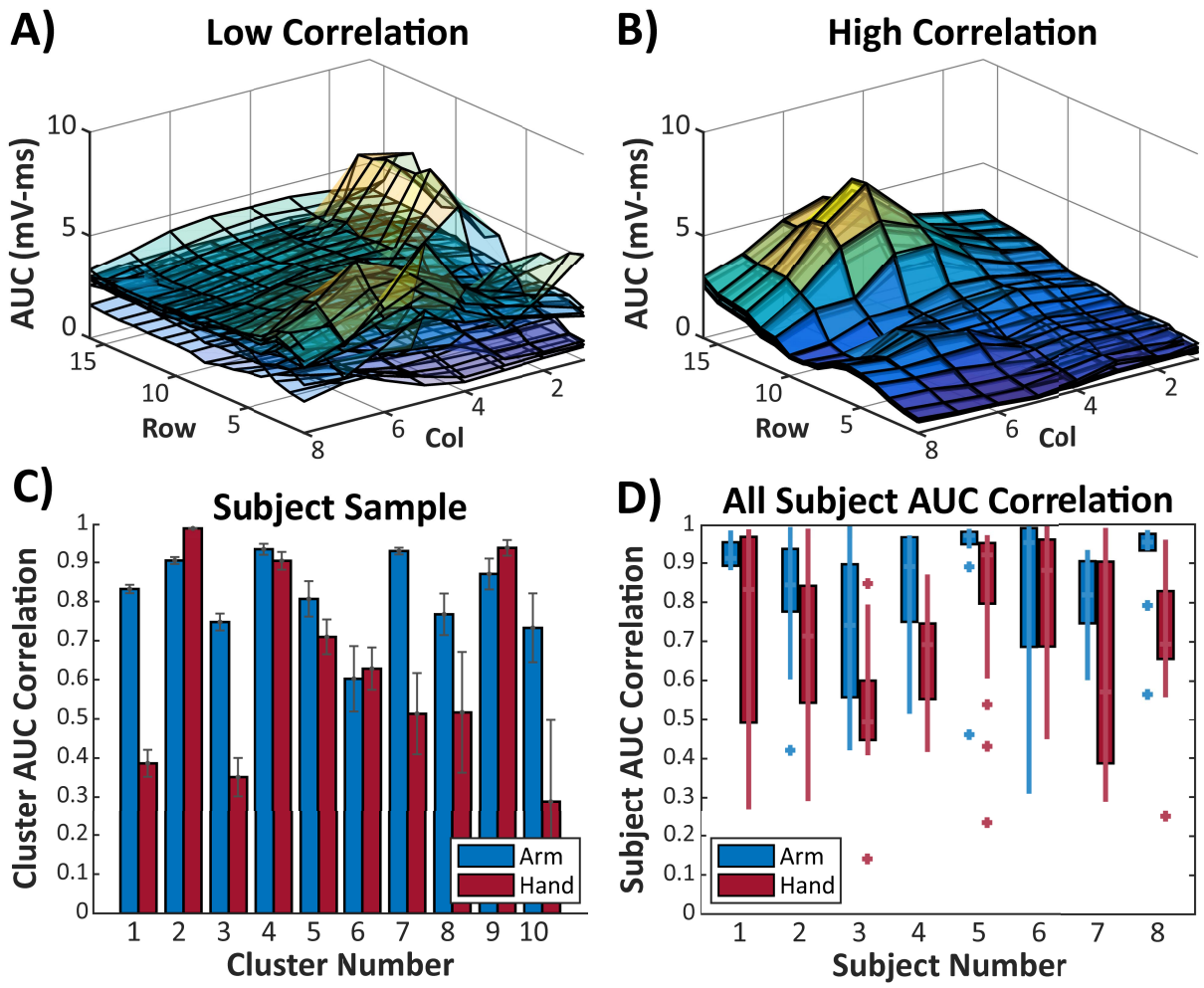

Fig. 6. AUC Correlation Samples and Distribution. A) Sample cluster with low EMG AUC correlation. B) Sample cluster with high EMG AUC correlation. C) AUC correlation average (and Standard Error Bars, gray)) from all arm and hand clusters from a single subject. D) AUC correlation of each subject for both arm and hand. The box represents the interquartile range, and the whiskers indicate $\pm 2.7\ \sigma$ of the cluster correlation values. Additional points indicate outliers.

multiple fingers. This behavior is functionally comparable to the natural coactivations of fingers related to grasp. Even for single finger tasks increased force inevitably recruits previously inactive finger muscles due to enslaving effects [32].

Another key point of the proximal nerve stimulation is the ability to activate both the intrinsic muscles in the hand and the extrinsic muscles in the forearm. For finger flexion, the intrinsic muscles in the hand controls the metacarpophalangeal joints, while the extrinsic muscles control the proximal and distal interphalangeal joints. For conventional NMES, muscle activation is specific to the site of the stimulation, and therefore a full prehension of the hand requires stimulation electrodes over both the intrinsic and extrinsic muscles [33], [34], but intrinsic muscles are not routinely targeted in clinical practice. In contrast, activation of the intrinsic muscles with the proximal electrode grid location is beneficial as one electrode location can elicit a full grasp motion. This is functionally significant as it enables the refinement of electrode selection to potentially target specific muscles for either a distal finger grasp or a palmar grasp depending on the task.

It is important to note that a higher AUC correlations in the arm was observed compared with the hand. This finding suggests that the EMG of the intrinsic hand muscles for a specific movement has more variation than its extrinsic arm counterparts. One contributing factor may be that, for a given force pattern, the stimulated nerve fibers may not elicit activity in the intrinsic muscles as regularly. Additionally, the smaller hand pad and smaller muscles may produce larger relative variations in the EMG output and AUC correlations. Further isolation and repetition of intrinsic finger specific activation patterns are necessary to better understand this behavior.

B. Activation Redundancy

The nerve stimulation grid also demonstrates a certain level of system redundancy in both the different electrode pairs available for a specific movement as well as the variation in muscle fiber activation that produces the same force. The redundancy of the stimulation system can be seen in the various set of similar forces that are generated from different

electrode pairs. Following the hierarchical clustering, force pattern clusters are formed from a set of electrode pairs and these clusters have a varying number of pairs (Figure 5). Each cluster represents a relatively distinct force profile that can be generated with multiple different stimulation locations. Functionally, these different electrode pairs could then be used as alternative options to produce the same desired force.

This redundancy in the stimulation system is valuable as it can enable different electrode pairs to be used during stimulation to produce the same force pattern. This can potentially reduce/delay the fatigue impact of the stimulation by interleaving the activation of different sets of nerve axons and muscle fibers. Additionally, these redundant electrode pairs are valuable in compensating for inherent system instability that can arise from underlying electrode-nerve movement or changes in electrode-skin contact. In addition to the variety of similar electrode pairs and forces, each cluster of forces also has varying EMG activations. The EMG AUC correlation was calculated as a measure of similarity or dissimilarity of the EMG activity elicited by the electrode locations within a cluster. As seen in Figure 6D, some subjects have force clusters with high AUC correlations, while others have a much wider range of correlation values. Both high and low AUC correlations suggest different physiological scenarios in muscle recruitment. A force cluster with high EMG AUC correlation suggests that the specific nerve fibers being activated by the electrode pairs innervate similar sets of muscle fibers recorded from the skin surface, although deep muscle fibers, outside of the recording range of our skin-surface electrode, can also be recruited. Alternatively, a force cluster with lower EMG AUC correlation suggests that the nerve fibers being activated innervate a more diffuse, non-overlapping set of muscle fibers. Functionally, since these sets of electrodes have similar force outputs, a desired force pattern could be generated by different sets of muscle fibers. However, the recorded finger forces only represent one dimensional force (normal force), the actual generated forces may be in different directions, which means the similar forces in a cluster can be directed to different directions. Therefore, the degree of redundancy may be limited.

C. Limitations

A limitation of the current methodology is the inter-session stability of the electrode placement and force output results. Although anatomical landmarks are used to ensure similar setup and grid placement, the same sets of movements and electrode pairs may not be exactly reproduced once the electrode grid is removed. Although the latent redundancy of the system suggests that similar force patterns are likely repeatable between grid placements, this still has the prerequisite of searching through all the electrode pairs for the available sets of forces. This procedure can be minimized down to quickly search for different active pairs for automated re-calibration. Future studies will also be completed to better quantify the difference of electrode placement and force patterns between sessions.

The current study was focused on the elicitable finger force patterns, another limitation is the potentially changing proportions of force at each finger that could occur with higher current levels, as seen in Figure 3. Even at the same electrode pair, it is possible that an increase in the stimulation current could result in the recruitment of nerve fibers which innervate different muscles, thereby leading to varying degrees of finger selectivity at different current levels. Although a single current-force relation was used to estimate the overall grid activity each electrode pair likely has its own current range and force stability. Further testing is necessary to better evaluate the stability of single electrode pairs in eliciting similar finger forces at different current levels.

Although this methodology is intended to help restore finger forces in individuals with muscle weakness, such as after stroke or spinal cord injury, it is important to note that control subjects tested in this study may have different muscle and body composition from that of the intended population. Secondly, motor impairment in SCI or stroke populations are not only characterized by paretic muscles, but also with spasticity or high muscle tone [35], [36]. In the current study, subjects were asked to relax while stimulation was delivered. In real application, subjects may not be able to relax the muscles voluntarily. Simultaneous stimulation for finger extension is necessary to counteract spasticity or to help with weakness in the finger extensors (more prevalent in stroke survivors) [37], [38]. A parallel exploration of radial nerve stimulation for finger and wrist extension has been performed using a similar technique [39]. Lastly, another important aspect in creating a functional grasp is the positioning and flexion of the thumb, which was not evaluated in this study. The practical concerns of obtaining all the necessary degrees of freedom with the existing finger force setup was the main barrier to this experimental decision. These aspects need to be integrated with the finger flexion stimulation for further evaluation of functional grasp patterns.

V. Conclusions

The current study utilized a grid of stimulation electrodes to stimulate the ulnar and median nerves, which produced a wide variety of finger flexion patterns. Our results showed that the system can elicit a number of multi-finger and single-finger activation patterns with a high level of redundancy to allow for multiple electrode pairs to be used for similar output forces. Moving forward, this automated stimulation system can be used as a foundation for a neuroprosthetic device for rehabilitation and functional assistance of individuals with hand weakness.

References

[1] C. E. Lang, M. D. Bland, R. R. Bailey, S. Y. Schaefer, and R. L. Birkenmeier, "Assessment of upper extremity impairment, function, and activity after stroke: Foundations for clinical decision making," *J. Hand Therapy*, vol. 26, no. 2, pp. 104–115, Apr. 2013.

[2] N. Scherbakov, S. von Haehling, S. D. Anker, U. Dirnagl, and W. Doehner, "Stroke induced sarcopenia: Muscle wasting and disability after stroke," *Int. J. Cardiol.*, vol. 170, pp. 89–94, Dec. 2013.

[3] J. W. Krakauer, "Arm function after stroke: From physiology to recovery," *Seminars Neurol.*, vol. 25, no. 4, pp. 384–395, 2005.

[4] C. K. Thomas, E. Y. Zaidner, B. Calancie, J. G. Broton, and B. R. Bigland-Ritchie, "Muscle weakness, paralysis, and atrophy after human cervical spinal cord injury," *Exp. Neurol.*, vol. 148, no. 2, pp. 414–423, 1997.

[5] K. D. Anderson, "Targeting recovery: Priorities of the spinal cord-injured population," *J. Neurotrauma*, vol. 21, no. 10, pp. 1371–1383, Oct. 2004.

[6] D. G. Kamper, H. C. Fischer, E. G. Cruz, and W. Z. Rymer, "Weakness is the primary contributor to finger impairment in chronic stroke," *Arch. Phys. Med. Rehabil.*, vol. 87, no. 9, pp. 1262–1269, 2006.

[7] P. H. Peckham and J. S. Knutson, "Functional electrical stimulation for neuromuscular applications," *Annu. Rev. Biomed. Eng.*, vol. 7, pp. 327–360, Feb. 2005.

[8] L. R. Sheffler and J. Chae, "Neuromuscular electrical stimulation in neurorehabilitation," *Muscle Nerve*, vol. 35, no. 5, pp. 562–590, 2007.

[9] B. M. Doucet, A. Lam, and L. Griffin, "Neuromuscular electrical stimulation for skeletal muscle function," *Yale J. Biol. Med.*, vol. 85, no. 2, pp. 201–215, 2012.

[10] K. Takeda, G. Tanino, and H. Miyasaka, "Review of devices used in neuromuscular electrical stimulation for stroke rehabilitation," *Med. Devices*, vol. 10, pp. 207–213, Aug. 2017.

[11] J. R de Kroon, M. Ijzerman, J. Chae, G. J. Lankhorst, and G. Zilvold, "Relation between stimulation characteristics and clinical outcome of the upper extremity in stroke," *J. Rehabil. Med.*, vol. 37, pp. 65–74, Apr. 2005.

[12] T. A. Thrasher, V. Zivanovic, W. Mcilroy, and M. R. Popovic, "Rehabilitation of reaching and grasping function in severe hemiplegic patients using functional electrical stimulation therapy," *Neurorehabilitation Neural Repair*, vol. 22, no. 6, pp. 706–714, 2008.

[13] F. Quandt and F. C. Hummel, "The influence of functional electrical stimulation on hand motor recovery in stroke patients: A review," *Exp. Transl. Stroke Med.*, vol. 6, Aug. 2014, Art. no. 9.

[14] N. Malešević *et al.*, "A multi-pad electrode based functional electrical stimulation system for restoration of grasp," *J. Neuroeng. Rehabil.*, vol. 9, no. 1, p. 66, 2012.

[15] A. D. Koutsou, J. C. Moreno, A. J. del Ama, E. Rocon, and J. L. Pons, "Advances in selective activation of muscles for non-invasive motor neuroprostheses," *J. Neuroeng. Rehabil.*, vol. 13, Jun. 2016, Art. no. 56.

[16] D. B. Popovic, "Advances in functional electrical stimulation (FES)," *J. Electromyogr. Kinesiol.*, vol. 24, pp. 795–802, Dec. 2014.

[17] A. Crema, N. Malešević, I. Furfaro, F. Raschellà, A. Pedrocchi, and S. Micera, "A wearable multi-site system for NMES-based hand function restoration," *IEEE Trans. Neural Syst. Rehabil. Eng.*, vol. 26, no. 2, pp. 428–440, Feb. 2018.

[18] A. J. Bergquist, J. M. Clair, and D. F. Collins, "Motor unit recruitment when neuromuscular electrical stimulation is applied over a nerve trunk compared with a muscle belly: Triceps surae," *J. Appl. Physiol.*, vol. 110, no. 3, pp. 627–637, 2011.

[19] A. J. Bergquist, M. J. Wiest, and D. F. Collins, "Motor unit recruitment when neuromuscular electrical stimulation is applied over a nerve trunk compared with a muscle belly: Quadriceps femoris," *J. Appl. Physiol.*, vol. 113, no. 1, pp. 78–89, 2012.

[20] A. J. Bergquist, M. J. Wiest, Y. Okuma, and D. F. Collins, "H-reflexes reduce fatigue of evoked contractions after spinal cord injury," *Muscle Nerve*, vol. 50, no. 2, pp. 224–234, 2014.

[21] H. Shin, Z. Watkins, and X. Hu, "Exploration of hand grasp patterns elicitable through non-invasive proximal nerve stimulation," *Sci. Rep.*, vol. 7, Nov. 2017, Art. no. 16595.

[22] H. Shin and X. Hu, "Flexibility of finger activation patterns elicited through non-invasive multi-electrode nerve stimulation," in *Proc. Annu. Int. Conf. IEEE Eng. Med. Biol. Soc.*, Jul. 2018, pp. 1428–1431.

[23] H. Shin, Y. Zheng, and X. Hu, "Variation of finger activation patterns post-stroke through non-invasive nerve stimulation," *Front. Neurol.*, vol. 9, p. 1101, Dec. 2018.

[24] Y. Zheng and X. Hu, "Improved muscle activation using proximal nerve stimulation with subthreshold current pulses at kilohertz-frequency," *J. Neural Eng.*, vol. 15, no. 4, 2018, Art. no. 046001.

[25] H. Shin, R. Chen, and X. Hu, "Delayed fatigue in finger flexion forces through transcutaneous nerve stimulation," *J. Neural Eng.*, vol. 15, no. 6, 2018, Art. no. 066005.

[26] Y. Zheng and X. Hu, "Reduced muscle fatigue using kilohertz-frequency subthreshold stimulation of the proximal nerve," *J. Neural Eng.*, vol. 15, no. 6, 2018, Art. no. 066010.

[27] Y. Zheng, H. Shin, and X. Hu, "Muscle fatigue post-stroke elicited from kilohertz-frequency subthreshold nerve stimulation," *Front. Neurol.*, vol. 9, p. 1061, Dec. 2018.

[28] C. Salchow-Hömmen *et al.*, "User-centered practicability analysis of two identification strategies in electrode arrays for FES induced hand motion in early stroke rehabilitation," *J. Neuroeng. Rehabil.*, vol. 15, Dec. 2018, Art. no. 123.

[29] B. Redmond, R. Aina, T. Gorti, and B. Hannaford, "Haptic characteristics of some activities of daily living," in *Proc. IEEE Haptics Symp.*, Mar. 2010, pp. 71–76.

[30] P. J. Rousseeuw, "Silhouettes: A graphical aid to the interpretation and validation of cluster analysis," *J. Comput. Appl. Math.*, vol. 20, no. 1, pp. 53–65, 1987.

[31] N. K. Fowler and A. C. Nicol, "Measurement of external three-dimensional interphalangeal loads applied during activities of daily living," *Clin. Biomech.*, vol. 14, pp. 646–652, Nov. 1999.

[32] V. M. Zatsiorsky, Z.-M. Li, and M. L. Latash, "Enslaving effects in multi-finger force production," *Exp. Brain Res.*, vol. 131, no. 2, pp. 187–195, Mar. 2000.

[33] U. Arnet, D. A. Muzykewicz, J. Fridén, and R. L. Lieber, "Intrinsic hand muscle function, part 1: Creating a functional grasp," *J. Hand Surg.*, vol. 38, pp. 2093–2099, Nov. 2013.

[34] D. A. Muzykewicz, U. Arnet, R. L. Lieber, and J. Fridén, "Intrinsic hand muscle function, part 2: Kinematic comparison of 2 reconstructive procedures," *J. Hand Surg.*, vol. 38, pp. 2100.e1–2105.e1, Nov. 2013.

[35] M. M. Adams and A. L. Hicks, "Spasticity after spinal cord injury," *Spinal Cord*, vol. 43, pp. 577–586, Apr. 2005.

[36] C. L. Watkins, M. J. Leathley, J. M. Gregson, A. P. Moore, T. L. Smith, and A. K. Sharma, "Prevalence of spasticity post stroke," *Clin. Rehabil.*, vol. 16, no. 5, pp. 515–522, 2002.

[37] D. G. Kamper, R. L. Harvey, S. Suresh, and W. Z. Rymer, "Relative contributions of neural mechanisms versus muscle mechanics in promoting finger extension deficits following stroke," *Muscle Nerve*, vol. 28, no. 3, pp. 309–318, Sep. 2003.

[38] C. E. Lang, S. L. DeJong, and J. A. Beebe, "Recovery of thumb and finger extension and its relation to grasp performance after stroke," *J. Neurophysiol.*, vol. 102, no. 1, pp. 451–459, 2009.

[39] Y. Zheng and X. Hu, "Elicited finger and wrist extension through transcutaneous radial nerve stimulation," *IEEE Trans. Neural Syst. Rehabil. Eng.*, vol. 27, no. 9, pp. 1875–1882, Sep. 2019.